

# 1 **CoproID predicts the source of coprolites 2 and paleofeces using microbiome 3 composition and host DNA content**

4 **Maxime Borry<sup>1</sup>, Bryan Cordova<sup>1</sup>, Angela Perri<sup>2, 11</sup>, Marsha C.  
5 Wibowo<sup>17, 18, 3</sup>, Tanvi Honap<sup>8, 16</sup>, Wing Tung Jada Ko<sup>4</sup>, Jie Yu<sup>5</sup>, Kate  
6 Britton<sup>11, 15</sup>, Linus Girdland Flink<sup>15, 19</sup>, Robert C. Power<sup>11, 12</sup>, Ingelise  
7 Stuijts<sup>13</sup>, Domingo Salazar Garcia<sup>14</sup>, Courtney A. Hofman<sup>8, 16</sup>, Richard W.  
8 Hagan<sup>1</sup>, Thérèse Samdapawindé Kagone<sup>6</sup>, Nicolas Meda<sup>6</sup>, Hélène  
9 Carabin<sup>7</sup>, David Jacobson<sup>8, 16</sup>, Karl Reinhard<sup>9</sup>, Cecil M. Lewis, Jr.<sup>8, 16</sup>,  
10 Aleksandar Kostic<sup>17, 18, 3</sup>, Choongwon Jeong<sup>1</sup>, Alexander Herbig<sup>1</sup>,  
11 Alexander Hübner<sup>1</sup>, and Christina Warinner<sup>1, 4, 10</sup>**

12 **<sup>1</sup>Department of Archaeogenetics, Max Planck Institute for the Science of Human  
13 History, Jena, Germany 07745**

14 **<sup>2</sup>Department of Archaeology, Durham University, Durham, UK DH13LE**

15 **<sup>3</sup>Harvard Medical School, Department of Microbiology, Boston, MA, USA 02215**

16 **<sup>4</sup>Department of Anthropology, Harvard University, Cambridge, MA, USA 02138**

17 **<sup>5</sup>Department of History, Wuhan University, Wuhan, China**

18 **<sup>6</sup>Centre MURAZ Research Institute/Ministry of Health, Bobo-Dioulasso, Burkina Faso**

19 **<sup>7</sup>Département de pathologie et de microbiologie, Faculté de Médecine**

20 **vétérinaire-Université de Montréal, Saint-Hyacinthe, Canada, QC J2S 2M2**

21 **<sup>8</sup>Department of Anthropology, University of Oklahoma, Norman, OK, USA 73019**

22 **<sup>9</sup>School of Natural Resources, University of Nebraska, Lincoln, NE, USA 68583**

23 **<sup>10</sup>Faculty of Biological Sciences, Friedrich-Schiller University, Jena, Germany, 07743**

24 **<sup>11</sup>Department of Human Evolution, Max Planck Institute for Evolutionary Anthropology,  
25 Leipzig, Germany**

26 **<sup>12</sup>Institut für Vor- und Frühgeschichtliche Archäologie und Provinzialrömische  
27 Archäologie, Ludwig-Maximilians-Universität München, Munich**

28 **<sup>13</sup>The Discovery Programme, 6 Mount Street Lower, Dublin 2, Ireland**

29 **<sup>14</sup>Grupo de Investigación en Prehistoria IT-622-13 (UPV- EHU), IKERBASQUE-Basque  
30 Foundation for Science**

31 **<sup>15</sup>Department of Archaeology, University of Aberdeen, St Mary's Building, Elphinstone  
32 Road, Aberdeen, AB24 3UF, UK**

33 **<sup>16</sup>Laboratories of Molecular Anthropology and Microbiome Research (LMAMR),  
34 University of Oklahoma, Norman, OK, USA 73019**

35 **<sup>17</sup>Joslin Diabetes Center, Section on Pathophysiology and Molecular Pharmacology,  
36 Boston, MA, USA**

37 **<sup>18</sup>Joslin Diabetes Center, Section on Islet Cell and Regenerative Biology, Boston, MA,  
38 USA**

39 **<sup>19</sup>School of Natural Sciences and Psychology, Liverpool John Moores University, L3  
40 3AF Liverpool, United Kingdom**

41 Corresponding author:

42 Maxime Borry, Christina Warinner

43 Email address: [borry@shh.mpg.de](mailto:borry@shh.mpg.de), [warinner@shh.mpg.de](mailto:warinner@shh.mpg.de)

## 44 **ABSTRACT**

45 Shotgun metagenomics applied to archaeological feces (paleofeces) can bring new insights into the  
46 composition and functions of human and animal gut microbiota from the past. However, paleofeces often  
47 undergo physical distortions in archaeological sediments, making their source species difficult to identify  
48 on the basis of fecal morphology or microscopic features alone. Here we present a reproducible and  
49 scalable pipeline using both host and microbial DNA to infer the host source of fecal material. We apply  
50 this pipeline to newly sequenced archaeological specimens and show that we are able to distinguish  
51 morphologically similar human and canine paleofeces, as well as non-fecal sediments, from a range of  
52 archaeological contexts.

## 53 INTRODUCTION

54 The gut microbiome, located in the distal colon and primarily studied through the analysis of feces,  
55 is the largest and arguably most influential microbial community within the body (Huttenhower et al.,  
56 2012). Recent investigations of the human microbiome have revealed that it plays diverse roles in  
57 health and disease, and gut microbiome composition has been linked to a variety of human health states,  
58 including inflammatory bowel diseases, diabetes, and obesity (Kho and Lal, 2018). To investigate the gut  
59 microbiome, metagenomic sequencing is typically used to reveal both the taxonomic composition (i.e.,  
60 which bacteria are there) and the functions the microbes are capable of performing (i.e., their potential  
61 metabolic activities) (Sharpton, 2014). Given the importance of the gut microbiome in human health, there  
62 is great interest in understanding its recent evolutionary and ecological history (Warinner and Lewis Jr,  
63 2015; Davenport et al., 2017).

64 Paleofeces, either in an organic or partially mineralized (coprolite) state, present a unique opportunity  
65 to directly investigate changes in the structure and function of the gut microbiome through time (Warinner  
66 et al., 2015). Paleofeces are found in a wide variety of archaeological contexts around the world and are  
67 generally associated with localized processes of dessication, freezing, or mineralization. Paleofeces can  
68 range in size from whole, intact fecal pieces (Jiménez et al., 2012) to millimeter-sized sediment inclusions  
69 identifiable by their high phosphate and fecal sterol content (Sistiaga et al., 2014). Although genetic  
70 approaches have long been used to investigate dietary DNA found within human (Gilbert et al., 2008;  
71 Poinar et al., 2001) and animal (Poinar et al., 1998; Hofreiter et al., 2000; Bon et al., 2012; Wood et al.,  
72 2016) paleofeces, it is only recently that improvements in metagenomic sequencing and bioinformatics  
73 have enabled detailed characterization of their microbial communities (Tito et al., 2008, 2012; Warinner  
74 et al., 2017).

75 However, before evolutionary studies of the gut microbiome can be conducted, it is first necessary  
76 to confirm the host source of the paleofeces under study. Feces can be difficult to taxonomically assign  
77 by morphology alone (Supplementary Note), and human and canine feces can be particularly difficult to  
78 distinguish in archaeological contexts (Poinar et al., 2009). Since their initial domestication more than  
79 12,000 years ago (Frantz et al., 2016), dogs have often lived in close association with humans, and it is not  
80 uncommon for human and dog feces to co-occur at archaeological sites. Moreover, dogs often consume  
81 diets similar to humans because of provisioning or refuse scavenging (Guiry, 2012), making their feces  
82 difficult to distinguish based on dietary contents. Even well-preserved fecal material degrades over time,  
83 changing in size, shape, and color (Figure 1). The combined analysis of host and microbial ancient DNA  
84 (aDNA) within paleofeces presents a potential solution to this problem.

85 Previously, paleofeces host source has been genetically inferred on the basis of PCR-amplified  
86 mitochondrial DNA sequences alone (Hofreiter et al., 2000); however, this is problematic in the case of  
87 dogs, which, in addition to being pets and working animals, were also eaten by many ancient cultures  
88 (Clutton-Brock and Hammond, 1994; Rosenswig, 2007; Kirch and O'Day, 2003; Podberscak, 2009), and  
89 thus trace amounts of dog DNA may be expected to be present in the feces of humans consuming dogs.  
90 Additionally, dogs often scavenge on human refuse, including human excrement (Butler and Du Toit,  
91 2002), and thus ancient dog feces could also contain trace amounts of human DNA, which could be  
92 further inflated by PCR-based methods.

93 A metagenomics approach overcomes these issues by allowing a quantitative assessment of eukaryotic  
94 DNA at a genome-wide scale, including the identification and removal of modern human contaminant

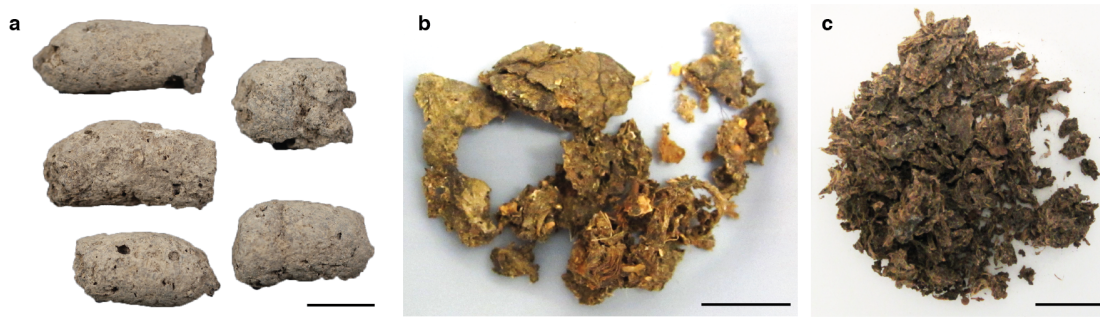


**Figure 1. Examples of archaeological paleofeces analyzed in this study.**

(a) H29-3, from Anhui Province, China, Neolithic period; (b) Zape 2, from Durango, Mexico, ca. 1300 BP; (c) Zape 28, from Durango, Mexico, ca. 1300 BP. Paleofeces ranged from slightly mineralized intact pieces (a) to more fragmentary organic states (b, c), and color ranged from pale gray (a) to dark brown (c). Each scale bar represents 2 cm.

95 DNA that could potentially arise during excavation or subsequent curation or storage. It also allows for the  
96 microbial composition of the feces to be taken into account. Gut microbiome composition differs among  
97 mammal species (Ley et al., 2008), and thus paleofeces microbial composition could be used to confirm and  
98 authenticate host assignment. Available microbial tools, such as SourceTracker (Knights et al., 2011) and  
99 FEAST (Shenhav et al., 2019), can be used to perform the source prediction of microbiome samples from  
100 uncertain sources (sinks) using a reference dataset of source-labeled microbiome samples and, respectively,  
101 Gibbs sampling or an Expectation-Maximization algorithm. However, although SourceTracker has been  
102 widely used for modern microbiome studies and has even been applied to ancient gut microbiome data  
103 (Tito et al., 2012) (Hagan et al., 2019), it was not designed to be a host species identification tool for  
104 ancient microbiomes.

105 In this work we present a bioinformatics method to infer and authenticate the host source of paleofeces  
106 from shotgun metagenomic DNA sequencing data: coproID (**coprolite IDentification**). coproID combines  
107 the analysis of putative host ancient DNA with a machine learning prediction of the feces source based  
108 on microbiome taxonomic composition. Ultimately, coproID predicts the host source of a paleofeces  
109 specimen from the shotgun metagenomic data derived from it. We apply coproID to previously published  
110 modern fecal datasets and show that it can be used to reliably predict their host. We then apply coproID to  
111 a set of newly sequenced paleofeces specimens and non-fecal archaeological sediments and show that  
112 it can discriminate between feces of human and canine origin, as well as between fecal and non-fecal  
113 samples.

## 114 MATERIAL AND METHODS

### 115 Gut microbiome reference datasets

116 Previously published modern reference microbiomes were chosen to represent the diversity of potential pa-  
117 leofeces sources and their possible contaminants, namely human fecal microbiomes from Non-Westernized  
118 Human/Rural (NWHR), and Westernized Human/Urban (WHU) communities, dog fecal microbiomes,  
119 and soil samples (Table 1). Because the human datasets had been filtered to remove human genetic  
120 sequences prior to database deposition, we additionally generated new sequencing data from 118 fe-  
121 cal specimens from both NWHR and WHU populations (Table S5) in order to determine the average  
122 proportion and variance of host DNA in human feces.

Metagenome source	Food production	N	Analysis	Source
Homo sapiens - USA	WHU	36	microbiome	The Human Microbiome Project Consortium et al. (2012)
Homo sapiens - India (Bhopal and Kerala)	WHU & NWHR	19	microbiome	Dhakam et al. (2019)
Homo sapiens - Fiji (agrarian villages)	NWHR	20	microbiome	Brito et al. (2019)
Homo sapiens - Madagascar	NWHR	110	microbiome	Pasolli et al. (2019)
Homo sapiens - Brazil (Yanomami)	NWHR	3	microbiome	Pasolli et al. (2019)
Homo sapiens - Peru (Tunapuco)	NWHR	12	microbiome	Obregon-Tito et al. (2015)
Homo sapiens - Tanzania (Hadza)	NWHR	38	microbiome	Rampelli et al. (2015)
Homo sapiens - Peru (Matses)	NWHR	24	microbiome	Obregon-Tito et al. (2015)
Homo sapiens - USA (Boston)	WHU	49	host DNA	This study
Homo sapiens - Burkina Faso	NWHR	69	host DNA	This study
Canis familiaris	-	150	microbiome and host DNA	Coelho et al. (2018)
Soil	-	16	microbiome	Fierer et al. (2012)
Soil	-	2	microbiome	CSIR and aromatic plants (2016)
Soil	-	2	microbiome	Orellana et al. (2018)

**Table 1. Modern reference microbiome datasets**

123 **Archaeological samples**

124 A total of 20 archaeological samples, originating from 10 sites and spanning periods from 7200 BP to the  
125 medieval era, were selected for this study. Among these 20 samples, of which 17 are newly sequenced, 13  
126 are paleofeces, 4 are midden sediments, and 3 are sediments obtained from human pelvic bone surfaces.  
127 (Table 2).

Archaeological ID	Laboratory ID	Site Name	Region	Period	Sample type	Archaeologically suspected species	Plot ID
Zape 2*	ZSM002	Cueva de los Muertos Chiquitos	Mexico	1300 BP	Paleofeces	HUMAN	01
Zape 5*	ZSM005	Cueva de los Muertos Chiquitos	Mexico	1300 BP	Paleofeces	HUMAN	02
Zape 23	ZSM023	Cueva de los Muertos Chiquitos	Mexico	1300 BP	Paleofeces	HUMAN or CANID	03
Zape 25	ZSM025	Cueva de los Muertos Chiquitos	Mexico	1300 BP	Paleofeces	HUMAN	04
Zape 27	ZSM027	Cueva de los Muertos Chiquitos	Mexico	1300 BP	Paleofeces	HUMAN	05
Zape 28*	ZSM028	Cueva de los Muertos Chiquitos	Mexico	1300 BP	Paleofeces	HUMAN	06
Zape 29	ZSM029	Cueva de los Muertos Chiquitos	Mexico	1300 BP	Paleofeces	HUMAN	07
Zape 31	ZSM031	Cueva de los Muertos Chiquitos	Mexico	1300 BP	Paleofeces	HUMAN	08
H29-1	AHP001	Xiaosungang	China	Neolithic 7200-6800 BP	Paleofeces	CANID or CERVID	09
H35-1	AHP002	Xiaosungang	China	Neolithic 7200-6800 BP	Paleofeces	CANID or CERVID	10
H29-2	AHP003	Xiaosungang	China	Neolithic 7200-6800 BP	Paleofeces	CANID or CERVID	11
H29-3	AHP004	Xiaosungang	China	Neolithic 7200-6800 BP	Paleofeces	CANID or CERVID	12
LG 4560.69	YRK001	Surrey	UK	Post-Medieval	Paleofeces	HUMAN	13
AP3-CL197S163	DRL001.A	Derragh	Ireland	Mesolithic	Midden Sediment	-	14
AP4-A6-2860	CBA001.A	Cabeço das Amoreiras	Portugal	Mesolithic	Midden Sediment	-	15
AP5-798-162	BRF001.A	Binchester Roman Fort	England	Roman	Midden Sediment	-	16
AP6-LPZ702	LEI010.A	Leipzig	Germany	10th- 11th century AD	Midden Sediment	-	17
AP7-6-28353	ECO004.D	El Collado	Spain	Mesolithic	Pelvic Sediment	-	18
AP8-CMN-M1	CMN001.D	Cingle del Mas Nou	Spain	Mesolithic	Pelvic Sediment	-	19
AP9-17590	MLP001.A	Molpir	Slovakia	7th century BC	Pelvic Sediment	-	20

\*Metagenomic data were previously published in (Hagan et al., 2019)

**Table 2. Archaeological samples**

## 128 **Sampling**

129 Paleofeces specimens from Mexico were sampled in a dedicated aDNA cleanroom in the Laboratories  
130 for Molecular Anthropology and Microbiome Research (LMAMR) at the University of Oklahoma, USA.  
131 Specimens from China were sampled in a dedicated aDNA cleanroom at the Max Planck Institute for  
132 the Science of Human History (MPI-SHH) in Jena, Germany. All other specimens were first sampled at  
133 the Max Planck Institute for Evolutionary Anthropology (MPI-EVA) in Leipzig, Germany before being  
134 transferred to the MPI-SHH for further processing. Sampling was performed using a sterile stainless  
135 steel spatula or scalpel, followed by homogenization in a mortar and pestle, if necessary. Because the  
136 specimens from Xiaosungang, China were very hard and dense, a rotary drill was used to section the  
137 coprolite prior to sampling. Where possible, fecal material was sampled from the interior of the specimen  
138 rather than the surface. Specimens from Molphir and Leipzig were received suspended in a buffer of  
139 trisodium phosphate, glycerol, and formyl following screening for parasite eggs using optical microscopy.  
140 For each paleofeces specimen, a total of 50-200 mg was analyzed.

141 Modern feces were obtained under informed consent from Boston, USA (WHU) (Wibowo et al., 2019)  
142 from a long-term (>50 years) type 1 diabetes cohort, and from villages in Burkina Faso (NWHR) as part  
143 of broader studies on human gut microbiome biodiversity and health-associated microbial communities.  
144 Feces were collected fresh and stored frozen until analysis. A total of 250 mg was analyzed for each fecal  
145 specimen,

## 146 **DNA Extraction**

147 For paleofeces and sediment samples, DNA extractions were performed using a silica spin column  
148 protocol (Dabney et al., 2013) with minor modifications in dedicated aDNA cleanrooms located at  
149 LMAMR (Mexican paleofeces) and the MPI-SHH (all other paleofeces). At LMAMR, the modifications  
150 followed those of protocol D described in (Hagan et al., 2019). DNA extractions at the MPI-SHH were  
151 similar, but omitted the initial bead-beating step, and a single silica column was used per sample instead of  
152 two. Additionally, to reduce centrifugation errors, DNA extractions performed at the MPI-SHH substituted  
153 the column apparatus from the High Pure Viral Nucleic Acid Large Volume Kit (Roche, Switzerland)  
154 in place of the custom assembled Zymo-reservoirs coupled to MinElute (Qiagen) columns described  
155 in (Dabney et al., 2013). At both locations, non-template negative extraction controls were processed  
156 alongside samples to identify and monitor potential contamination.

157 For modern feces, DNA was extracted from Burkina Faso fecal samples using the AllPrep PowerViral  
158 DNA/RNA Qiagen kit at Centre MURAZ Research Institute in Burkina Faso. DNA was extracted from  
159 the Boston fecal material using the ZymoBIOMICS DNA Miniprep Kit (D4303) at the Joslin Diabetes  
160 Center as described in (Wibowo et al., 2019).

## 161 **Library preparation and Sequencing**

162 For paleofeces and sediment samples, double-stranded, dual-indexed shotgun Illumina libraries were  
163 constructed following (Meyer and Kircher, 2010) using either the NEBNext DNA Library Prep Master  
164 Set (E6070) kit (Hagan et al., 2019; Mann et al., 2018) for the Mexican paleofeces or individually  
165 purchased reagents (Mann et al., 2018) for all other samples. Following library amplification using a  
166 Kapa HiFi Uracil+ polymerase or Agilent Pfu Turbo Cx Hotstart polymerase, the libraries were purified  
167 using a Qiagen MinElute PCR Purification kit and quantified using either a BioAnalyzer 2100 with High  
168 Sensitivity DNA reagents or an Agilent Tape Station D1000 Screen Tape kit. The Mexican libraries  
169 were pooled in equimolar amounts and sequenced on an Illumina HiSeq 2000 using 2x100 bp paired-end  
170 sequencing. All other libraries were pooled in equimolar amounts and sequenced on an Illumina HiSeq  
171 4000 using 2x75 bp paired-end sequencing.

172 For modern NWHR feces, double-stranded, dual-indexed shotgun Illumina libraries were constructed  
173 in a dedicated modern DNA facility at LMAMR. Briefly, after DNA quantification using a Qubit dsDNA  
174 Broad Range Assay Kit, DNA was sheared using a QSonica Q800R in 1.5mL 4°C cold water at 50%  
175 amplitude for 12 minutes to aim for a fragment size between 400 and 600 bp. Fragments shorter than  
176 150 bp were removed using Sera-Mag SpeedBeads and a Alpaqua 96S Super Magnet Plate. End-repair  
177 and A-tailing was performed using the Kapa HyperPrep EndRepair and A-Tailing Kit, and Illumina  
178 sequencing adapters were added. After library quantification, libraries were dual-indexed in an indexing  
179 PCR over four replicates, pooled, and purified using the SpeedBeads. Libraries were quantified using  
180 the Agilent Fragment Analyzer, pooled in equimolar ratios, and size-selected using the Pippin Prep to  
181 a target size range of 400-600 bp. Libraries were sequenced on an Illumina NovaSeq S1 using 2x150

182 bp paired-end sequencing at the Oklahoma Medical Research Foundation Next-Generation Sequencing  
183 Core facility. Modern WHU libraries were generated using the NEBNext DNA library preparation kit  
184 following manufacturer's recommendations, after fragmentation by shearing for a target fragment size of  
185 350 bp as described in (Wibowo et al., 2019). The libraries were then pooled and sequenced by Novogene  
186 on a NovaSeq S4 using 2x150 bp paired-end sequencing.

### 187 **Proportion of host DNA in gut microbiome**

188 Because it is standard practice to remove human DNA sequences from metagenomics DNA sequence files  
189 before data deposition into public repositories, we were unable to infer the proportion of human DNA  
190 in human feces from publicly available data. To overcome this problem, we measured the proportion  
191 of human DNA in two newly generated fecal metagenomics datasets from Burkina Faso (NWHR) and  
192 Boston, U.S.A. (WHU) (Table S5). To measure the proportion of human DNA in each fecal dataset,  
193 we used the Anonymap pipeline (Borry, 2019a) to perform a mapping with Bowtie 2 (Langmead and  
194 Salzberg, 2012) with the parameters `--very-sensitive -N 1` after adapter cleaning and reads  
195 trimming for ambiguous and low-quality bases with a QScore below 20 by AdapterRemoval v2 (Schubert  
196 et al., 2016). To preserve the anonymity of the donors, the sequences of mapped reads were then replaced  
197 by Ns thus anonymizing the alignment files. We obtained the proportion of host DNA per sample by  
198 dividing the number of mapped reads by the total number of reads in the sample. The proportion of host  
199 DNA in dog feces was determined from the published dataset Coelho et al. (2018) as described above, but  
200 without the anonymization step.

### 201 **coproID pipeline**

202 Data were processed using the coproID pipeline v1.0 (Figure 2) (DOI: 10.5281/zenodo.2653757) written  
203 using Nextflow (Di Tommaso et al., 2017) and made available through nf-core (Ewels et al., 2019).  
204 Nextflow is a Domain Specific Language designed to ensure reproducibility and scalability for scientific  
205 pipelines, and nf-core is a community-developed set of guidelines and tools to promote standardization  
206 and maximum usability of Nextflow pipelines.

207 coproID consists of 5 different steps:

#### 208 **Preprocessing**

209 *Fastq* sequencing files are given as an input. After quality control analysis with FastQC (Andrews et al.,  
210 2010), raw sequencing reads are cleaned from sequencing adapters and trimmed from ambiguous and  
211 low-quality bases with a QScore below 20, while reads shorter than 30 base pairs are discarded using  
212 AdapterRemoval v2. By default, paired-end reads are merged on overlapping base pairs.

#### 213 **Mapping**

214 The preprocessed reads are then aligned to each of the target species genomes (source species) by Bowtie2  
215 with the `--very-sensitive` preset while allowing for a mismatch in the seed search (`-N 1`).

216 When running coproID with the ancient DNA mode (`--adna`), alignments are filtered by PMDtools  
217 (Skoglund et al., 2014) to only retain reads showing post-mortem damages (PMD). PMDtools default  
218 settings are used, with specified library type, and only reads with a PMDScore greater than three are kept.

#### 219 **Computing host DNA content**

220 Next, filtered alignments are processed in Python using the Pysam library (pysam developers, 2018).  
221 Reads matching above the identity threshold of 0.95 to multiple host genomes are flagged as common  
222 reads  $reads_{common}$  whereas reads mapping above the identity threshold to a single host genome are  
223 flagged as genome-specific host reads  $reads_{spec\ g}$  to each genome  $g$ . Each source species host DNA is  
224 normalized by genome size and gut microbiome host DNA content such as:

$$NormalizedHostDNA(source\ species) = \frac{\sum length(reads_{spec\ g})}{genome_g\ length \cdot endo_g} \quad (1)$$

225 where for each species of genome  $g$ ,  $\sum length(reads_{spec\ g})$  is the total length of all  $reads_{spec\ g}$ ,  
226  $genome_g\ length$  is the size of the genome, and  $endo_g$  is the host DNA proportion in the species gut  
227 microbiome.

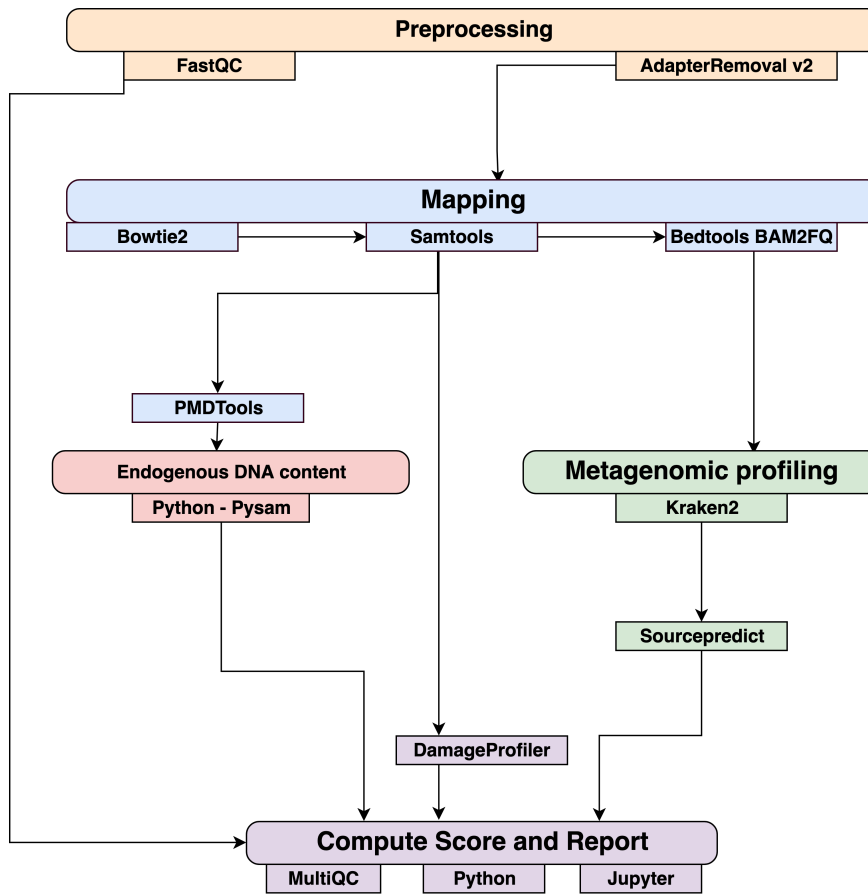


**Figure 2. Workflow schematic of the coproID pipeline.**

coproID consists of five steps: *Preprocessing* (orange), *Mapping* (blue), *Computing host DNA content for each metagenome* (red), *Metagenomic profiling* (green), and *Reporting* (violet). Individual programs (squared boxes) are colored by category (rounded boxes)

228 Afterwards, an host DNA ratio is computed for each source species such as:

$$NormalizedRatio(\text{source species}) = \frac{NormalizedHostDNA(\text{source species})}{\sum NormalizedHost DNA (\text{source species})} \quad (2)$$

229 where  $\sum NormalizedHost DNA (\text{source species})$  is the sum of all source species Normalized Host  
230 DNA.

#### 231 **Metagenomic profiling**

232 Adapter clipped and trimmed reads are given as an input to Kraken 2 (Wood and Salzberg, 2014). Using  
233 the MiniKraken2\_v2\_8GB database ( 2019/04/23 version), Kraken 2 performs the taxonomic classification  
234 to output a taxon count per sample report file. All samples taxon count are pooled together in a taxon  
235 counts matrix with samples in columns, and taxons in rows. Next, Sourcepredict (Borry, 2019b) is used to  
236 predict the source based on each microbiome sample taxon composition. Using dimension reduction and  
237 K-Nearest Neighbors (KNN) machine learning trained with reference modern gut microbiomes samples  
238 (Table 1), Sourcepredict estimates a proportion  $prop_{microbiome}(\text{source species})$  of each potential source  
239 species, here Human or Dog, for each sample.

#### 240 **Reporting**

For each filtered alignment file, the DNA damage patterns are estimated with DamageProfiler (Peltzer and Neukamm, 2019). The information from the host DNA content and the metagenomic profiling are

gathered for each source in each sample such as:

$$\text{proportion}(\text{source species}) = \text{NormalizedRatio}(\text{source species}) \cdot \text{prop}_{\text{microbiome}}(\text{source species})$$

241 Finally, a summary report is generated including the damage plots, a summary table of the coproID  
242 metrics, and the embedding of the samples in two dimensions by Sourcepredict. coproID is available on  
243 GitHub at the following address: [github.com/nf-core/coproid](https://github.com/nf-core/coproid).

## 244 RESULTS

245 We analyzed 21 archaeological samples with coproID v1.0 to estimate their source using both host DNA  
246 and microbiome composition.

### 247 Host DNA in reference gut microbiomes

248 Before analyzing the archaeological samples, we first tested whether there is a per-species difference in  
249 host DNA content in modern reference human and dog feces. With Anonymap, we computed the amount  
250 of host DNA in each reference gut microbiome (Table S1). We found that the median percentages of  
251 host DNA in NWHR, WHU, and Dog (Figure 3) are significantly different at  $\alpha = 0.05$  (Kruskal-  
252 Wallis H-test = 117.40, p value < 0.0001). We confirmed that there is a significant difference of median  
253 percentages of host DNA between dogs and NWHR, as well as dogs and WHU, with Mann-Whitney U  
254 tests (Table 3) and therefore corrected each sample by the mean percentage of gut host DNA found in  
255 each species, 1.24% for humans ( $\mu_{\text{NWHR}} = 0.85$ ,  $\sigma_{\text{NWHR}} = 2.33$ ,  $\mu_{\text{WHU}} = 1.67$ ,  $\sigma_{\text{WHU}} = 0.81$ ), and 0.11%  
256 for dogs ( $\sigma_{\text{dog}} = 0.16$ ) (equation 1, table S1). This information was used to correct for the amount of host  
257 DNA found in paleofeces.

Comparison	Mann-Whitney U test	p value
Dog vs NWHR	3327.0	< 0.0001
Dog vs WHU	41.0	< 0.0001
NWHR vs WHU	370.0	< 0.0001
Dog vs Human	3368.0	< 0.0001

**Table 3.** Statistical comparison of reference gut host DNA content. Mann-Whitney U test for independent observations.  $H_0$ : the distributions of both populations are equal.

### 258 The effect of PMD filtering on host species prediction

259 Because aDNA accumulates damage over time (Briggs et al., 2007), we could use this characteristic to  
260 filter for reads carrying these specific damage patterns using PMDtools, and therefore reduce modern  
261 contamination in the dataset. We applied PMD filtering to our archaeological datasets, and for each,  
262 compared the predicted host source before and afterwards. The predicted host sources did not change after  
263 the DNA damage read filtering, but some became less certain (Figure 4). Most samples are confidently  
264 assigned to one of the two target species, however some samples previously categorized as humans now lie  
265 in the uncertainty zone. This suggests that PMDtools filtering lowered the modern human contamination  
266 which might have originated from sample excavation and manipulation.

267 The trade-off of PMDtools filtering is that it reduces the assignment power by lowering the number  
268 of reads available for host DNA based source prediction by only keeping PMD-bearing reads. This  
269 loss is greater for well-preserved samples, which may have relatively few damaged reads (< 15% of  
270 total). Ultimately, applying damage filtering can make it more difficult to categorize samples on the sole  
271 basis of host DNA content, but it also makes source assignments more reliable by removing modern  
272 contamination.

### 273 Source microbiome prediction of reference samples by Sourcepredict

274 To help resolve ambiguities related to the host aDNA present within a sample, we also investigated gut  
275 microbiome composition as an additional line of evidence to better predict paleofeces source. After  
276 performing taxonomic classification using Kraken2, we computed a sample pairwise distance matrix from  
277 the species counts. With the t-SNE dimension reduction method, we embedded this distance matrix in

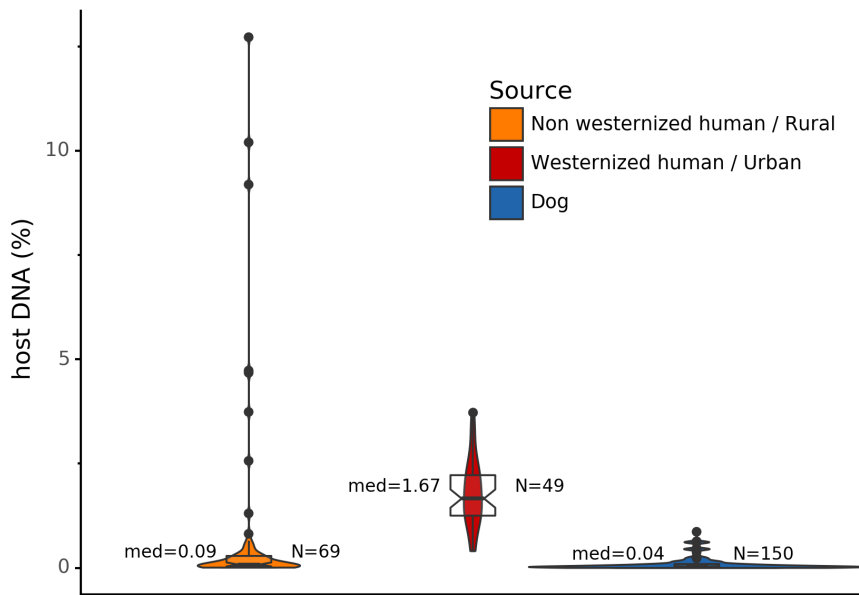


**Figure 3. Gut microbiome host DNA content.**

The median percentage of host DNA in the gut microbiome and the number of samples in each group are displayed besides each boxplot.

278 two dimensions to visualize the sample positions and sources (Figure 5a). We then used a KNN machine  
279 learning classifier on this low dimension embedding to predict the source of gut microbiome samples.  
280 This trained KNN model reached a test accuracy of 0.94 on previously unseen data (figure 5b).

#### 281 **Embedding of archaeological samples by Sourcepredict**

282 We used this trained KNN model to predict the sources of the 20 paleofeces and coprolite archaeological  
283 samples, after embedding them in a two-dimensional space (Figure 6). Based on their microbiome  
284 composition data, Sourcepredict predicted 2 paleofeces samples as dogs, 8 paleofeces samples as human,  
285 2 paleofeces samples and 4 archaeological sediments as soil, while the rest were predicted as unknown  
286 (Table S2).

#### 287 **coproID prediction**

288 Combining both PMD-filtered host DNA information and microbiome composition, coproID was able  
289 to reliably categorize 7 of the 13 paleofeces samples, as 5 human paleofeces and 2 canine paleofeces,  
290 whereas all of the non-fecal archaeological sediments were flagged as unknown. (Figure 8). This  
291 confirms the original archaeological source hypothesis for five samples (ZSM005, ZSM025, ZSM027,  
292 ZSM028, ZSM031) and specifies or rejects the original archaeological source hypothesis for the two  
293 others (YRK001, AHP004). The 6 paleofeces samples not reliably identified by coproID have a conflicting  
294 source proportion estimation between host DNA and microbiome composition (Figure 7a and 7b and  
295 Table S3). Specifically, paleofeces AHP001, AHP002, and AHP003 show little predicted gut microbiome  
296 preservation, and thus have likely been altered by taphonomic (decomposition) processes. Paleofeces  
297 ZSM002, ZSM023, and ZSM029, by contrast, show good evidence of both host and microbiome  
298 preservation, but have conflicting source predictions based on host and microbiome evidence. Given that  
299 subsistence is associated with gut microbiome composition, this conflict may be related to insufficient gut  
300 microbiome datasets available for non-Westernized dog populations (Hagan et al., 2019).

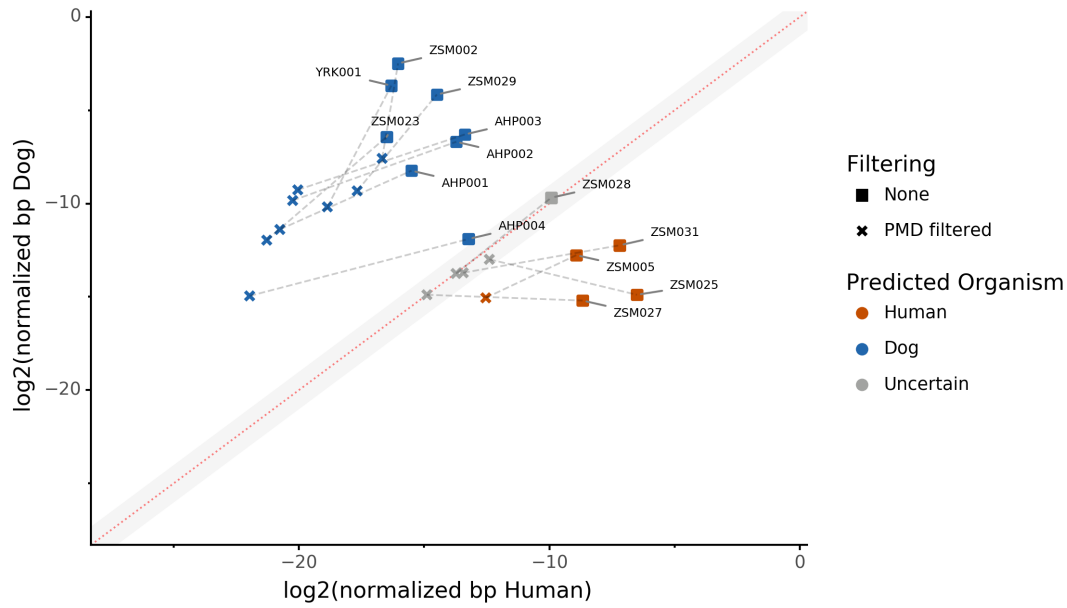


**Figure 4. The effect of filtering for damaged reads using PMD.**

The log<sub>2</sub> of the human *NormalizedHostDNA* is graphed against the log<sub>2</sub> of the dog *NormalizedHostDNA*. Squares represent samples before filtering by PMD, whereas crosses represent samples after filtering by PMD. Dotted lines show the correspondence between samples. The red diagonal line marks the boundary between the two species, and the grey shaded area indicates a zone of species uncertainty ( $\pm 1 \log_2 FC$ ) due to insufficient genetic information.

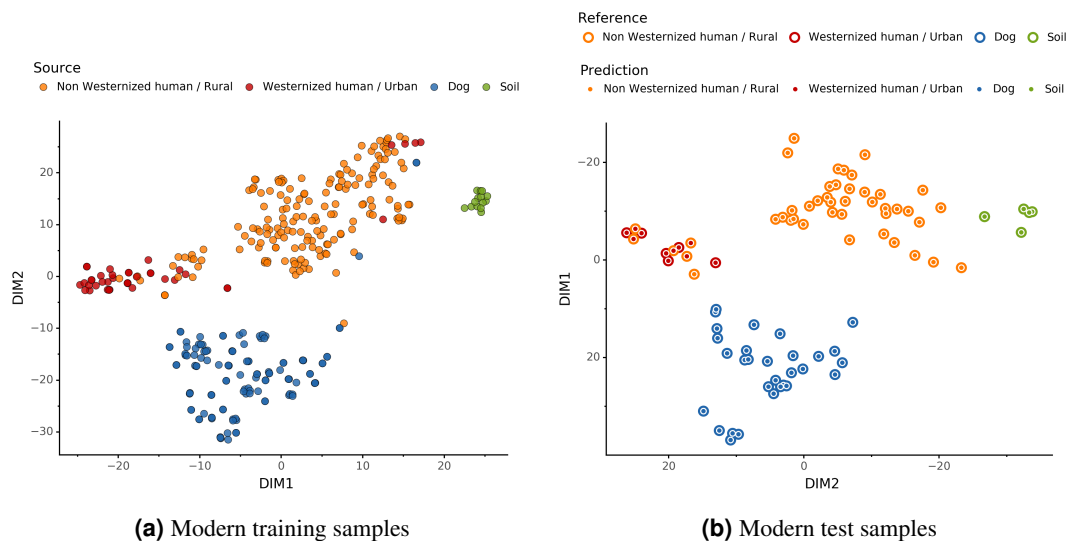


**Figure 5. Embedding of reference modern gut microbiomes.**

(a) t-SNE embedding of the species composition based on sample pairwise Weighted Unifrac distances for training modern gut microbiomes training samples. Samples are colored by their actual source. (b) t-SNE embedding of the species composition based on sample pairwise Weighted Unifrac distances for source prediction of modern test samples. The outer circle color is the actual source of a sample, while the inner circle color is the predicted sample source by Sourcepredict.

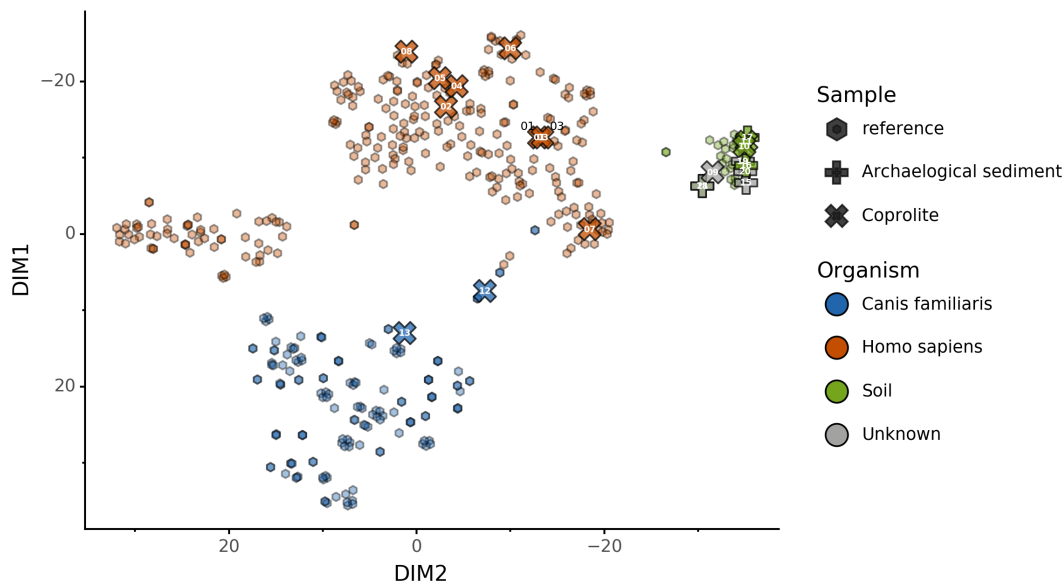


**Figure 6. Prediction of archaeological samples sources and t-SNE embedding by Sourcepredict.**  
t-SNE embedding of archaeological (crosses) and modern (hexagons) samples. The color of the modern samples is based on their actual source while the color of the archaeological samples is based on their predicted source by Sourcepredict. Archaeological sample are labelled with their *Plot ID* (Table 2).

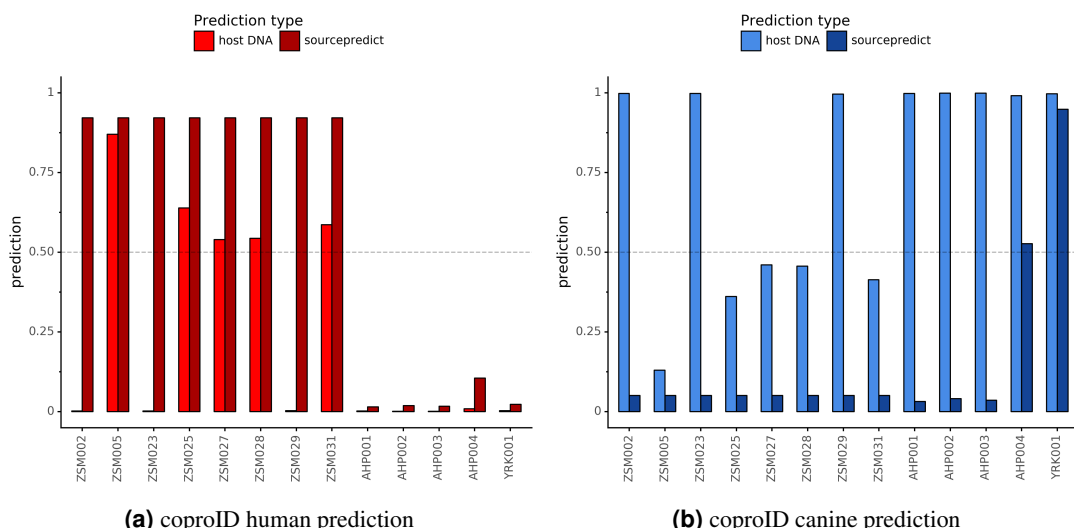


**Figure 7. Host DNA and Sourcepredict source prediction for paleofeces samples.** The vertical bar represents the predicted proportion by host DNA (lighter fill) or by Sourcepredict (darker fill). The horizontal dashed line represents the confidence threshold to assign a source to a sample.

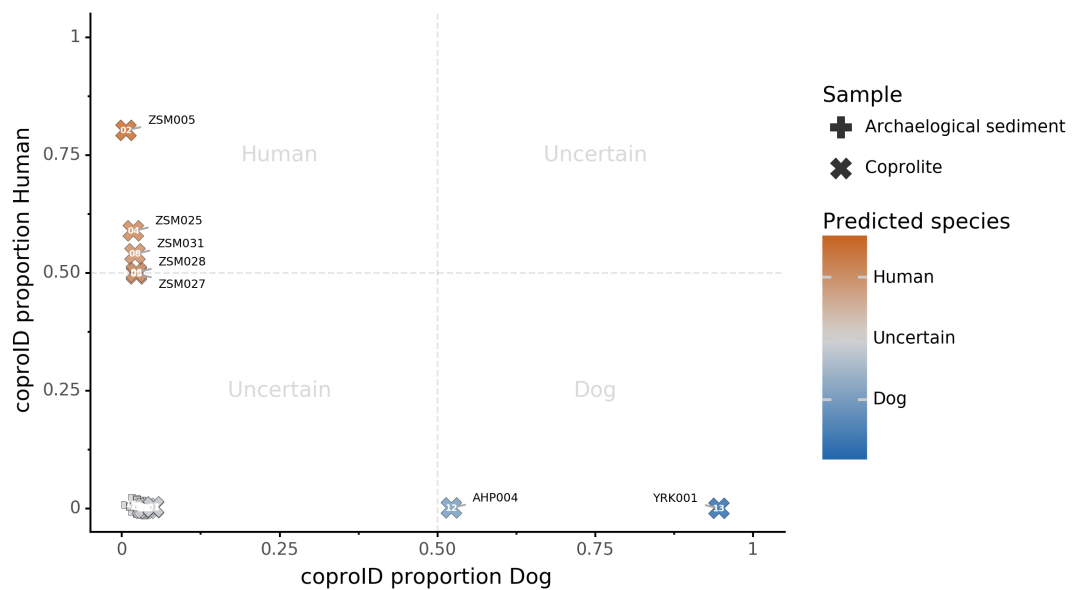


**Figure 8. coproID source prediction.**

Predicted human proportion graphed versus predicted canine proportion. Samples are colored by their predicted sources proportions. Samples with a low canine and human proportion are not annotated.

## 301 DISCUSSION

302 Paleofeces are the preserved remains of human or animal feces, and although they typically only preserve  
303 under highly particular conditions, they are nevertheless widely reported in the paleontological and  
304 archaeological records and include specimens ranging in age from the Paleozoic era (Dentzien-Dias et al.,  
305 2013) to the last few centuries. Paleofeces can provide unprecedented insights into animal health and  
306 diet, parasite biology and evolution, and the changing ecology and evolution of the gut microbiome.  
307 However, because many paleofeces lack distinctive morphological features, determining the host origin of  
308 a paleofeces can be a difficult problem (Poinar et al., 2009). In particular, distinguishing human and canine  
309 paleofeces can be challenging because they are often similar in size and shape, they tend to co-occur  
310 at archaeological sites and in midden deposits, and humans and domesticated dogs tend to eat similar  
311 diets (Guiry, 2012). We developed coproID to aid in identifying the source organism of archaeological  
312 paleofeces and coprolites by applying a combined approach relying on both ancient host DNA content  
313 and gut microbiome composition.

314 coproID addresses several shortcomings of previous methods. First, we have included a DNA damage-  
315 filtering step that allows for the removal of potentially contaminating modern human DNA, which may  
316 otherwise skew host species assignment. We have additionally measured and accounted for significant  
317 differences in the mean proportion of host DNA found in dog and human feces, and we also accounted for  
318 differences in host genome size between humans and dogs when making quantitative comparisons of host  
319 DNA. Then, because animal DNA recovered from paleofeces may contain a mixture of host and dietary  
320 DNA, we also utilize gut microbiome compositional data to estimate host source. We show that humans  
321 and dogs have distinct gut microbiome compositions, and that their feces can be accurately distinguished  
322 from each other and from non-feces using a machine learning classifier after data dimensionality reduction.  
323 Taken together, these approaches allow a robust determination of paleofeces and coprolite host source, that  
324 takes into account both modern contamination, microbiome composition, and postmortem degradation.

325 In applying coproID to a set of 20 archaeological samples of known and/or suspected origin, all  
326 7 non-fecal sediment samples were accurately classified as "uncertain" and were grouped with soil  
327 by Sourcepredict. For the 13 paleofeces and coprolites under study, 7 exhibited matching host and  
328 microbiome source assignments and were confidently classified as either human (n=5) or canine (n=2).  
329 Importantly, one of the samples confidently identified as canine was YRK001, a paleofeces that had been  
330 recovered from an archaeological chamber pot in the United Kingdom, but which showed an unusual  
331 diversity of parasites inconsistent with human feces, and therefore posed issues in host assignation.

332 For the remaining six unidentified paleofeces, three exhibited poor microbiome preservation and were  
333 classified as "uncertain", while the other three were well-preserved but yielded conflicting host DNA  
334 and microbiome assignments. These three samples, ZSM002, Z023, and ZSM029, all from prehistoric  
335 Mexico, all contain high levels of canine DNA, but have gut microbiome profiles within the range of  
336 NWHR humans. Classified as "uncertain", there are two possible explanations for these samples. First,  
337 these feces could have originated from a human who consumed a recent meal of canine meat. Dogs  
338 were consumed in ancient Mesoamerica (Clutton-Brock and Hammond, 1994; Santley and Rose, 1979;  
339 Rosenswig, 2007; Wing, 1978), but further research on the expected proportion of dietary DNA in human  
340 feces is needed to determine whether this is a plausible explanation for the very high amounts of canine  
341 DNA (and negligible amounts of human DNA) observed.

342 Alternatively, these feces could have originated from a canine whose microbiome composition is  
343 shifted relative to that of the reference metagenomes used in our training set. It is now well-established  
344 that subsistence mode strongly influences gut microbiome composition in humans Obregon-Tito et al.  
345 (2015), with NWHR and WHU human populations largely exhibiting distinct gut microbiome structure,  
346 as seen in (Figure 5a. To date, no gut microbiome data is available from non-Westernized dogs, and all  
347 reference dog metagenome data included as training data for coproID originated from a single study of  
348 labrador retrievers and beagles Coelho et al. (2018). Future studies of non-Westernized rural dogs are  
349 needed to establish the full range of gut microbial diversity in dogs and to more accurately model dog gut  
350 microbiome diversity in the past. Given that all confirmed human paleofeces in this study falls within  
351 the NWHR cluster (Figure 6), we anticipate that our ability to accurately classify dog paleofeces and  
352 coprolites as canine (as opposed to "uncertain") will improve with the future addition of non-Westernized  
353 rural dog metagenomic data.

## 354 CONCLUSIONS

355 We developed an open-source, documented, tested, scalable, and reproducible method to perform the  
356 identification of archaeological paleofeces and coprolite source. By leveraging the information from  
357 host DNA and microbiome composition, we were able to identify and/or confirm the source of newly  
358 sequenced paleofeces. We demonstrated that coproID can provide useful assistance to archaeologists in  
359 identifying authentic paleofeces and inferring their host. Future work on dog gut microbiome diversity,  
360 especially among rural, non-Westernized dogs, may help improve the tool's sensitivity even further.

## 361 ACKNOWLEDGMENTS

362 We thank David Petts, Zdeněk Tvrď, Susanne Stegmann-Rajtár, and Zuzana Rajtarova for contributing  
363 archaeological samples to this study. We thank the Guildford Museum (Guildford Borough Council  
364 Heritage Service) and Catriona Wilson for allowing us to analyze the chamber pot paleofeces sample  
365 from Surrey, UK. The sample from Derragh, Ireland was excavated by Discovery Programme, an all-  
366 Ireland public center of archaeological research supported by the Heritage Council, during field work  
367 in 2003 to 2005 as part of the Lake Settlement Project. This work was supported by the US National  
368 Institutes of Health R01GM089886 (to C.W. and C.M.L.), the Deutsche Forschungsgemeinschaft EXC  
369 2051 #390713860 (to C.W.), and the Max Planck Society. Author contributions were as follows: M.B.  
370 and C.W. designed the research. B.C., M.C.W., D.J., C.A.H., and R.W.H. performed the laboratory  
371 experiments. M.B., C.J., M.C.W., and T.H. analyzed the data. M.B. developed the bioinformatics tools  
372 and pipelines. C.W., K.R., K.B., L.G.F., A.P., A.K., W.T.J.K., R.P., I.S., D.S.G., J.Y., T.S.K., N.M., H.C.,  
373 and C.M.L. provided materials and resources. C.W., A.He., and A.Hü. supervised the research. M.B.  
374 wrote the article, with input from C.W., A.Hü., KR and the other co-authors.

## 375 DATA AND CODE AVAILABILITY

376 Genetic data are available in the European Nucleotide Archive (ERA) under the accessions PRJEB33577  
377 and PRJEB35362. The code for the analysis is available at [github.com/maxibor/coproid-article](https://github.com/maxibor/coproid-article).

## 378 REFERENCES

379 Andrews, S. et al. (2010). Fastqc: a quality control tool for high throughput sequence data.  
380 Bon, C., Berthonaud, V., Maksud, F., Labadie, K., Poulain, J., Artiguenave, F., Wincker, P., Aury, J.-M.,  
381 and Elalouf, J.-M. (2012). Coprolites as a source of information on the genome and diet of the cave  
382 hyena. *Proceedings of the Royal Society B: Biological Sciences*, 279(1739):2825–2830.  
383 Borry, M. (2019a). maxibor/anonymap: Anonymap v1.0.  
384 Borry, M. (2019b). Sourcepredict: Prediction of metagenomic sample sources using dimension reduction  
385 followed by machine learning classification. *Journal of Open Source Software*, 4(41):1540.  
386 Briggs, A. W., Stenzel, U., Johnson, P. L. F., Green, R. E., Kelso, J., Prüfer, K., Meyer, M., Krause, J.,  
387 Ronan, M. T., Lachmann, M., and Pääbo, S. (2007). Patterns of damage in genomic DNA sequences  
388 from a Neandertal. *Proceedings of the National Academy of Sciences*, 104(37):14616–14621.  
389 Brito, I. L., Gurry, T., Zhao, S., Huang, K., Young, S. K., Shea, T. P., Naisilisili, W., Jenkins, A. P., Jupiter,  
390 S. D., Gevers, D., and Alm, E. J. (2019). Transmission of human-associated microbiota along family  
391 and social networks. *Nature Microbiology*, page 1.  
392 Butler, J. and Du Toit, J. (2002). Diet of free-ranging domestic dogs (*canis familiaris*) in rural zimbabwe:  
393 implications for wild scavengers on the periphery of wildlife reserves. In *Animal Conservation forum*,  
394 volume 5, pages 29–37. Cambridge University Press.  
395 Clutton-Brock, J. and Hammond, N. (1994). Hot dogs: comestible canids in preclassic maya culture at  
396 cuello, belize. *Journal of Archaeological Science*, 21(6):819–826.  
397 Coelho, L. P., Kultima, J. R., Costea, P. I., Fournier, C., Pan, Y., Czarnecki-Maulden, G., Hayward, M. R.,  
398 Forslund, S. K., Schmidt, T. S. B., Descombes, P., Jackson, J. R., Li, Q., and Bork, P. (2018). Similarity  
399 of the dog and human gut microbiomes in gene content and response to diet. *Microbiome*, 6(1):72.  
400 CSIR, C. i. o. m. and aromatic plants (2016). *Chrysopogon zizanioides* (ID 322597) - BioProject - NCBI.  
401 Dabney, J., Knapp, M., Glocke, I., Gansauge, M.-T., Weihmann, A., Nickel, B., Valdiosera, C., García,  
402 N., Pääbo, S., Arsuaga, J.-L., et al. (2013). Complete mitochondrial genome sequence of a middle

403      pleistocene cave bear reconstructed from ultrashort dna fragments. *Proceedings of the National*  
404      *Academy of Sciences*, 110(39):15758–15763.

405      Davenport, E. R., Sanders, J. G., Song, S. J., Amato, K. R., Clark, A. G., and Knight, R. (2017). The  
406      human microbiome in evolution. *BMC biology*, 15(1):127.

407      Dentzien-Dias, P. C., Poinar Jr, G., de Figueiredo, A. E. Q., Pacheco, A. C. L., Horn, B. L., and Schultz,  
408      C. L. (2013). Tapeworm eggs in a 270 million-year-old shark coprolite. *PLoS One*, 8(1):e55007.

409      Dhakan, D. B., Maji, A., Sharma, A. K., Saxena, R., Pulikkan, J., Grace, T., Gomez, A., Scaria, J., Amato,  
410      K. R., and Sharma, V. K. (2019). The unique composition of Indian gut microbiome, gene catalogue,  
411      and associated fecal metabolome deciphered using multi-omics approaches. *GigaScience*, 8(3).

412      Di Tommaso, P., Chatzou, M., Floden, E. W., Barja, P. P., Palumbo, E., and Notredame, C. (2017).  
413      Nextflow enables reproducible computational workflows. *Nature biotechnology*, 35(4):316.

414      Ewels, P., Peltzer, A., Fillinger, S., Alneberg, J., Patel, H., Wilm, A., Garcia, M., Di Tommaso, P., and  
415      Nahnse, S. (2019). nf-core: Community curated bioinformatics pipelines. *bioRxiv*, page 610741.

416      Fierer, N., Leff, J. W., Adams, B. J., Nielsen, U. N., Bates, S. T., Lauber, C. L., Owens, S., Gilbert,  
417      J. A., Wall, D. H., and Caporaso, J. G. (2012). Cross-biome metagenomic analyses of soil micro-  
418      bial communities and their functional attributes. *Proceedings of the National Academy of Sciences*,  
419      109(52):21390–21395.

420      Frantz, L. A., Mullin, V. E., Pionnier-Capitan, M., Lebrasseur, O., Ollivier, M., Perri, A., Linderholm,  
421      A., Mattiengeli, V., Teasdale, M. D., Dimopoulos, E. A., et al. (2016). Genomic and archaeological  
422      evidence suggest a dual origin of domestic dogs. *Science*, 352(6290):1228–1231.

423      Gilbert, M. T. P., Jenkins, D. L., Götherstrom, A., Naveran, N., Sanchez, J. J., Hofreiter, M., Thomsen,  
424      P. F., Binladen, J., Higham, T. F., Yohe, R. M., et al. (2008). Dna from pre-clovis human coprolites in  
425      oregon, north america. *Science*, 320(5877):786–789.

426      Guiry, E. J. (2012). Dogs as analogs in stable isotope-based human paleodietary reconstructions: a review  
427      and considerations for future use. *Journal of Archaeological Method and Theory*, 19(3):351–376.

428      Hagan, R. W., Hofman, C. A., Hübner, A., Reinhard, K., Schnorr, S., Lewis, C. M., Sankaranarayanan,  
429      K., and Warinner, C. G. (2019). Comparison of extraction methods for recovering ancient microbial  
430      dna from paleofeces. *American Journal of Physical Anthropology*.

431      Hofreiter, M., Poinar, H. N., Spaulding, W. G., Bauer, K., Martin, P. S., Possnert, G., and Pääbo, S.  
432      (2000). A molecular analysis of ground sloth diet through the last glaciation. *Molecular Ecology*,  
433      9(12):1975–1984.

434      Huttenhower, C., Gevers, D., Knight, R., Abubucker, S., Badger, J. H., Chinwalla, A. T., Creasy, H. H.,  
435      Earl, A. M., FitzGerald, M. G., Fulton, R. S., et al. (2012). Structure, function and diversity of the  
436      healthy human microbiome. *nature*, 486(7402):207.

437      Jiménez, F. A., Gardner, S. L., Araújo, A., Fugassa, M., Brooks, R. H., Racz, E., and Reinhard, K. J.  
438      (2012). Zoonotic and human parasites of inhabitants of cueva de los muertos chiquitos, rio zape valley,  
439      durango, mexico. *Journal of Parasitology*, 98(2):304–310.

440      Kho, Z. Y. and Lal, S. K. (2018). The human gut microbiome—a potential controller of wellness and  
441      disease. *Frontiers in microbiology*, 9.

442      Kirch, P. and O'Day, S. J. (2003). New archaeological insights into food and status: a case study from  
443      pre-contact hawaii. *World Archaeology*, 34(3):484–497.

444      Knights, D., Kuczynski, J., Charlson, E. S., Zaneveld, J., Mozer, M. C., Collman, R. G., Bushman, F. D.,  
445      Knight, R., and Kelley, S. T. (2011). Bayesian community-wide culture-independent microbial source  
446      tracking. *Nature Methods*, 8(9):761–763.

447      Langmead, B. and Salzberg, S. L. (2012). Fast gapped-read alignment with bowtie 2. *Nature methods*,  
448      9(4):357.

449      Ley, R. E., Hamady, M., Lozupone, C., Turnbaugh, P. J., Ramey, R. R., Bircher, J. S., Schlegel, M. L.,  
450      Tucker, T. A., Schrenzel, M. D., Knight, R., et al. (2008). Evolution of mammals and their gut microbes.  
451      *Science*, 320(5883):1647–1651.

452      Mann, A. E., Sabin, S., Ziesemer, K., Vågene, Å. J., Schroeder, H., Ozga, A. T., Sankaranarayanan,  
453      K., Hofman, C. A., Yates, J. A. F., Salazar-García, D. C., et al. (2018). Differential preservation of  
454      endogenous human and microbial dna in dental calculus and dentin. *Scientific reports*, 8(1):9822.

455      Meyer, M. and Kircher, M. (2010). Illumina sequencing library preparation for highly multiplexed target  
456      capture and sequencing. *Cold Spring Harbor Protocols*, 2010(6):pdb-prot5448.

457      Obregon-Tito, A. J., Tito, R. Y., Metcalf, J., Sankaranarayanan, K., Clemente, J. C., Ursell, L. K.,

458 Zech Xu, Z., Van Treuren, W., Knight, R., Gaffney, P. M., Spicer, P., Lawson, P., Marin-Reyes, L.,  
459 Trujillo-Villarroel, O., Foster, M., Guija-Poma, E., Troncoso-Corzo, L., Warinner, C., Ozga, A. T., and  
460 Lewis, C. M. (2015). Subsistence strategies in traditional societies distinguish gut microbiomes. *Nature  
461 Communications*, 6:6505.

462 Orellana, L. H., Chee-Sanford, J. C., Sanford, R. A., Löffler, F. E., and Konstantinidis, K. T. (2018).  
463 Year-Round Shotgun Metagenomes Reveal Stable Microbial Communities in Agricultural Soils and  
464 Novel Ammonia Oxidizers Responding to Fertilization. *Applied and Environmental Microbiology*,  
465 84(2):e01646–17.

466 Pasolli, E., Asnicar, F., Manara, S., Zolfo, M., Karcher, N., Armanini, F., Beghini, F., Manghi, P., Tett,  
467 A., Ghensi, P., Collado, M. C., Rice, B. L., DuLong, C., Morgan, X. C., Golden, C. D., Quince,  
468 C., Huttenhower, C., and Segata, N. (2019). Extensive Unexplored Human Microbiome Diversity  
469 Revealed by Over 150,000 Genomes from Metagenomes Spanning Age, Geography, and Lifestyle.  
470 *Cell*, 176(3):649–662.e20.

471 Peltzer, A. and Neukamm, J. (2019). Integrative-Transcriptomics/DamageProfiler: DamageProfiler v0.4.7.

472 Podberscek, A. L. (2009). Good to pet and eat: The keeping and consuming of dogs and cats in south  
473 korea. *Journal of Social Issues*, 65(3):615–632.

474 Poinar, H., Fiedel, S., King, C. E., Devault, A. M., Bos, K., Kuch, M., and Debruyne, R. (2009). Comment  
475 on “DNA from pre-clovis human coprolites in oregon, north america”. *Science*, 325(5937):148–148.

476 Poinar, H. N., Hofreiter, M., Spaulding, W. G., Martin, P. S., Stankiewicz, B. A., Bland, H., Evershed,  
477 R. P., Possnert, G., and Pääbo, S. (1998). Molecular coproscopy: dung and diet of the extinct ground  
478 sloth *nothrotheriops shastensis*. *Science*, 281(5375):402–406.

479 Poinar, H. N., Kuch, M., Sobolik, K. D., Barnes, I., Stankiewicz, A. B., Kuder, T., Spaulding, W. G.,  
480 Bryant, V. M., Cooper, A., and Pääbo, S. (2001). A molecular analysis of dietary diversity for three  
481 archaic native americans. *Proceedings of the National Academy of Sciences*, 98(8):4317–4322.

482 pysam developers (2018). Pysam: a python module for reading and manipulating files in the sam/bam  
483 format.

484 Rampelli, S., Schnorr, S., Consolandi, C., Turroni, S., Severgnini, M., Peano, C., Brigidi, P., Crittenden,  
485 A., Henry, A., and Candela, M. (2015). Metagenome Sequencing of the Hadza Hunter-Gatherer Gut  
486 Microbiota. *Current Biology*, 25(13):1682–1693.

487 Rosenswig, R. M. (2007). Beyond identifying elites: Feasting as a means to understand early middle  
488 formative society on the pacific coast of mexico. *Journal of Anthropological Archaeology*, 26(1):1–27.

489 Santley, R. S. and Rose, E. K. (1979). Diet, nutrition and population dynamics in the basin of mexico.  
490 *World Archaeology*, 11(2):185–207.

491 Schubert, M., Lindgreen, S., and Orlando, L. (2016). Adapterremoval v2: rapid adapter trimming,  
492 identification, and read merging. *BMC research notes*, 9(1):88.

493 Sharpton, T. J. (2014). An introduction to the analysis of shotgun metagenomic data. *Frontiers in plant  
494 science*, 5:209.

495 Shenhav, L., Thompson, M., Joseph, T. A., Briscoe, L., Furman, O., Bogumil, D., Mizrahi, I., Pe'er, I.,  
496 and Halperin, E. (2019). FEAST: fast expectation-maximization for microbial source tracking. *Nature  
497 Methods*, page 1.

498 Sistiaga, A., Mallol, C., Galván, B., and Summons, R. E. (2014). The neanderthal meal: a new perspective  
499 using faecal biomarkers. *PloS one*, 9(6):e101045.

500 Skoglund, P., Northoff, B. H., Shunkov, M. V., Derevianko, A. P., Pääbo, S., Krause, J., and Jakobsson, M.  
501 (2014). Separating endogenous ancient DNA from modern day contamination in a Siberian Neandertal.  
502 *Proceedings of the National Academy of Sciences*, 111(6):2229–2234.

503 The Human Microbiome Project Consortium, Huttenhower, C., Gevers, D., Knight, R., Rob, W. O., et al.  
504 (2012). Structure, function and diversity of the healthy human microbiome. *Nature*, 486(7402):207–214.

505 Tito, R. Y., Knights, D., Metcalf, J., Obregon-Tito, A. J., Cleeland, L., Najar, F., Roe, B., Reinhard, K.,  
506 Sobolik, K., Belknap, S., Foster, M., Spicer, P., Knight, R., and Lewis, C. M. (2012). Insights from  
507 Characterizing Extinct Human Gut Microbiomes. *PLoS ONE*, 7(12):e51146.

508 Tito, R. Y., Macmil, S., Wiley, G., Najar, F., Cleeland, L., Qu, C., Wang, P., Romagne, F., Leonard, S.,  
509 Ruiz, A. J., et al. (2008). Phylotyping and functional analysis of two ancient human microbiomes.  
510 *PLoS One*, 3(11):e3703.

511 Warinner, C., Herbig, A., Mann, A., Fellows Yates, J. A., Weiß, C. L., Burbano, H. A., Orlando, L., and  
512 Krause, J. (2017). A robust framework for microbial archaeology. *Annual review of genomics and*

513        *human genetics*, 18:321–356.

514        Warinner, C. and Lewis Jr, C. M. (2015). Microbiome and health in past and present human populations.  
515        *American Anthropologist*, 117(4):740–741.

516        Warinner, C., Speller, C., Collins, M. J., and Lewis Jr, C. M. (2015). Ancient human microbiomes.  
517        *Journal of human evolution*, 79:125–136.

518        Wibowo, M. C., Yang, Z., Tierney, B. T., Luber, J. M., Barajas-Olmos, F., Cecilia, C.-C., Humberto,  
519        G.-O., Martinez-Hernandez, A., Zimmerman, S., Smile, F. E., Ballal, S. A., Reinhard, K., Russ, J.,  
520        Orozco, L., Snow, M., LeBlanc, S., and Kostic, A. D. (2019). Reconstruction of ancient microbial  
521        genomes from the human gut - in review. in review.

522        Wing, E. S. (1978). *Use of dogs for food: An adaptation to the coastal environment*. Elsevier.

523        Wood, D. E. and Salzberg, S. L. (2014). Kraken: ultrafast metagenomic sequence classification using  
524        exact alignments. *Genome biology*, 15(3):R46.

525        Wood, J. R., Crown, A., Cole, T. L., and Wilmshurst, J. M. (2016). Microscopic and ancient dna profiling  
526        of polynesian dog (kurī) coprolites from northern new zealand. *Journal of Archaeological Science: Reports*, 6:496–505.

527